NWL Technical Report TR-2737
April 1972

ULTRASONIC IMAGING OF CYLINDRICAL EXPLOSIVE LOADS

Carol E. Springer

Surface Warfare Department
Naval Weapons Laboratory

UNCLASSIFIED

Security Classification

DOCUMENT CONTROL DATA - R & D

Security classification of title, body of abstract and indexing annotation must be entered when the overall report is classified

1 ORIGINATING ACTIVITY (Corporate author)	2a. REPORT SECURITY CLASSIFICATION
Naval Weapons Laboratory Dahlgren, Virginia 22448	UNCLASSIFIED 2b. GROUP

3 REPORT TITLE

ULTRASONIC IMAGING OF CYLINDRICAL EXPLOSIVE LOADS

4 DESCRIPTIVE NOTES (Type of report and inclusive dates)

5 AUTHOR(S) (First name, middle initial, last name)

Carol E. Springer

6 REPORT DATE	7a. TOTAL NO OF PAGES	7b. NO OF REFS
April 1972		

8a CONTRACT OR GRANT NO	9a. ORIGINATOR'S REPORT NUMBER(S)
b. PROJECT NO	NWL TR-2737
c.	9b. OTHER REPORT NO(S) (Any other numbers that may be assigned this report)
d.	

10 DISTRIBUTION STATEMENT

Approved for public release: distribution unlimited.

11 SUPPLEMENTARY NOTES	12 SPONSORING MILITARY ACTIVITY

13 ABSTRACT

Acoustic holography has been used successfully to image a simulant of the explosive PBXW106. Flaws less than 1/8 inch can be detected in glass bead simulants which are 1/2 inch in thickness, using a frequency of 1 MH_z at 300 watts peak power. With these results, calculations were made which show that the explosive can be imaged. Flaws and density differences in the explosive can be determined at or near this same frequency.

An outline of a total, automated inspection system is given with detailed descriptions of the linear receiving array and the sonifying phased array. The liquid surface system currently being used for a research tool is also described.

DD FORM 1 NOV 65 1473 (PAGE 1)

S/N 0101-807-6801

UNCLASSIFIED

Security Classification

FOREWORD

The present work was prepared in support of the nondestructive testing program for the five inch improved projectile. The feasibility of using acoustic holography for real time, nondestructive testing of the explosive billet was investigated. Results confirmed the calculations performed and further development work on a total automated inspection system is being carried out.

The author thanks the staff of Holosonics for their cooperation in preparation of the data presented.

This report was reviewed by Dr. M. F. Rose, Head of the Research Group, Ballistics Division and Mr. L. M. Williams, III, Head of the Ballistics Division.

Released by:

J. E. COLVARD, Head,
Surface Warfare Department

ABSTRACT

Acoustic holography has been used successfully to image a simulant of the explosive PBXW106. Flaws less than 1/8 inch can be detected in glass bead simulants which are 1/2 inch in thickness, using a frequency of 1 MHz at 300 watts peak power. With these results, calculations were made which show that the explosive can be imaged. Flaws and density differences in the explosive can be determined at or near this same frequency.

An outline of a total, automated inspection system is given with detailed descriptions of the linear receiving array and the sonifying phased array. The liquid surface system currently being used for a research tool is also described.

TABLE OF CONTENTS

SECTION I

INTRODUCTION

Acoustic holography has been used to successfully image simulant of the explosive PBXW106. The simulated explosive billets were cylindrically shaped. The test was designed to determine power levels and frequencies necessary to inspect a granular, urethane based material for flaws of under 1/8 inch in size as well as density differences.

Although the simulant was mainly designed to show applicability of acoustic imaging to explosive inspection, the tests also show the wide applicability of the method in other fields and to other materials. The applications of acoustic imaging are discussed in Section VII. They range through the fields of weaponry, non-destructive testing, metallography, undersea detection and medicine. Work in all fields is still in the research stages. Improvements must be made in existing systems with available technology and further research is necessary to develop systems with better resolution and more sensitivity. Research of this type is being carried out at the Naval Weapons Laboratory.

SECTION II

TECHNICAL DESCRIPTION

Acoustic holography is a method of imaging the internal structure of an object either in two or three dimensions. A liquid is used as the transport medium for ultrasound in the megacycle range. The sound passes from the sending transducer through the test object and is focused by an acoustic lense onto either a liquid surface or a receiving transducer.

If a liquid surface is used, the object beam is compared to an acoustic reference beam also focused on the liquid surface at an angle, θ, to the object beam, as shown in FIGURE 2.1. Information is extracted from the ripple pattern on the liquid surface by obtaining the phase difference between the object and reference beam using reflected laser light. This ripple pattern image is the acoustic hologram. From it, a real time image is reproduced and can be displayed on a viewing screen.

If a receiving transducer is used, the object beam is focused directly on the transducer as shown in FIGURE 2.2. The receiving transducer is in the form of a single mosaic or an array. The reference beam is electronically simulated by a voltage, either constant or pulsed in synchronization with the object beam. Information is obtained from the receiving transducer in the form of voltage differences from each element of the mosaic or array. The voltage difference is produced when the object beam exerts pressure on the receiving transducer face. The mechanical pressure wave is converted to a voltage by the ceramic or quartz transducer. This voltage is then compared to the reference beam voltage. In the case of the pulsed reference beam, both amplitude and phase information is obtained. The information is extracted in the form of voltage differences and is processed to form the hologram. From the hologram, the object image is reproduced and displayed, again on a viewing screen.

In either the liquid surface or receiving transducer case, the acoustic beam can be focused on any plane within the object being observed. The penetration depth and resolution depend on the frequency of the ultrasound in the liquid surface case, and on the frequency and the size of the mosaic or array elements in the case of the receiving transducer.

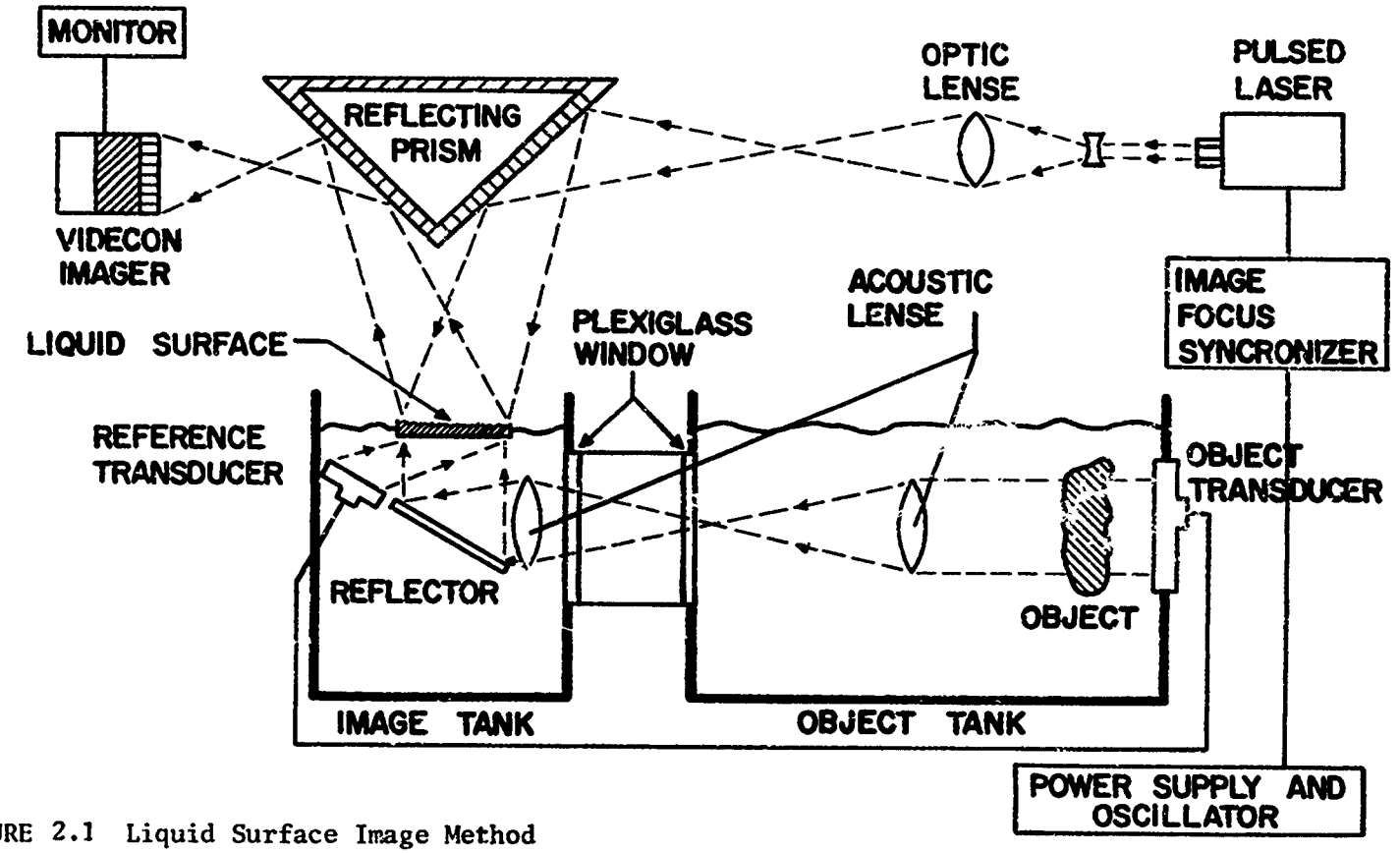

FIGURE 2.1 Liquid Surface Image Method

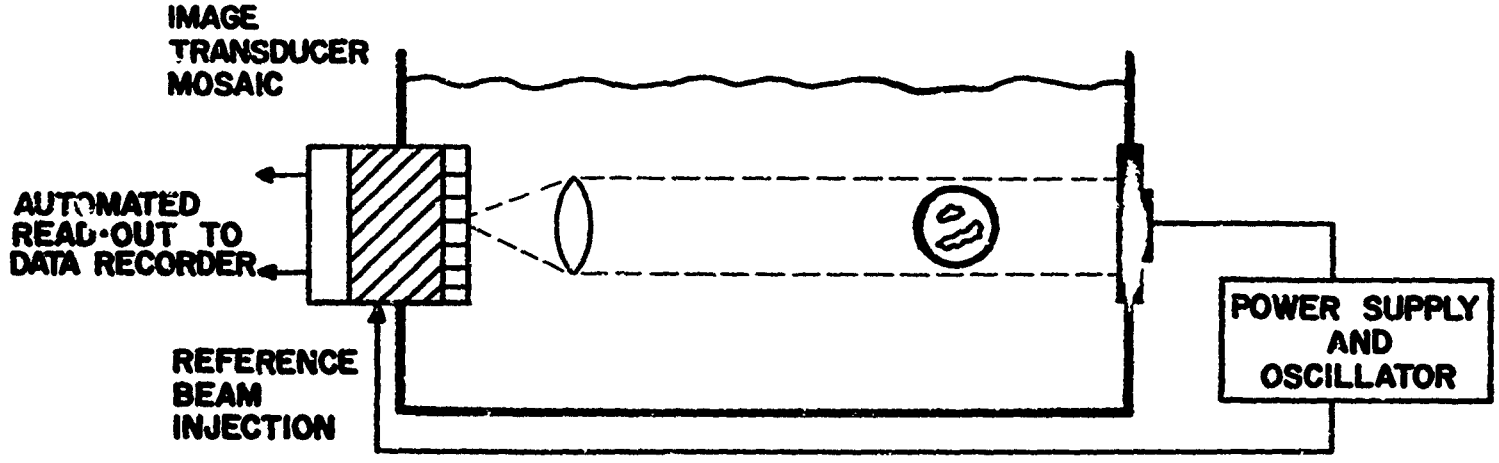

FIGURE 2.2. Non-Liquid Surface Imaging Method

SECTION III

PROGRAM FOR STUDY OF IMAGABLE OBJECTS

Before specifications for flaw detection in any object can be determined, it is necessary to investigate the imaging characteristics of the object. Consideration of the material, component parts and design characteristics is important. In the case of the 5-inch projectile, two materials must be studied, the explosive billet and the metal casing. Imaging characteristics of cylindrical, metal objects using holography are well known [1,2]. Thus the first phase of the program for imaging the 5-inch projectile is divided in two parts:

I. Feasibility of imaging the explosive billet alone

   A. Determination of the frequency necessary for an acceptable image and proper resolution

   B. Determination of the compatibility of the transport liquid and the explosive

II. Feasibility of imaging the explosive encased in the metal shell

   A. Determination of structure and material faults within the metal shell

   B. Interface studies of the bond between the explosive and the metal case along the cylinder walls, the tapered end and the base

A total inspection system for the 5-inch projectile is desired. Phase two of the program concerns the design of such a system.

III. Automation

   A. Design and production of a receiving transducer system, a sending array, a variable focus lense and a scan mechanism

   B. Design of an operator free rejection system for projectiles not meeting specifications. This is to be coupled with a permanent record of data pertinent to each projectile and a visual image of each.

   C. Design of an automated loading system for the projectiles compatible with the test equipment

A conceptual drawing of a system such as that described is shown in FIGURE 3.1.

Acoustic holography is a versatile tool for the nondestructive testing industry not only for gross imaging at the lower frequencies, but also for small resolution at the higher frequencies. The possibility of using the system designed for the 5 inch projectile in other nondestructive testing applications will be considered. In particular, high frequency capability of an acoustic system will be studied. This would be an aid in metal structure analysis. Three dimensional imaging of test objects will be considered. If additional information can be obtained from a three dimensional image, work in this area will be furthered.

The first phase of the study has been partially completed and design work has been started in phase two. The results are given in the following sections.

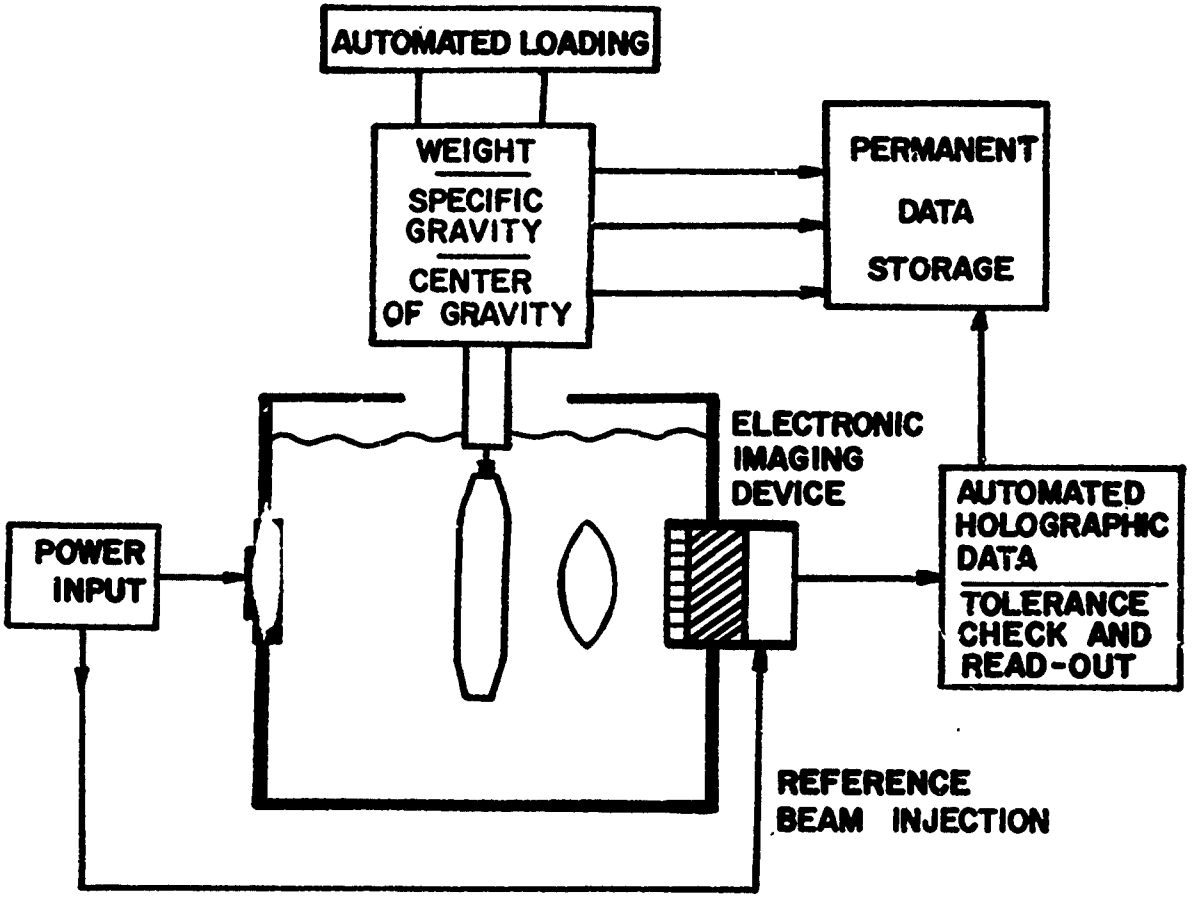

FIGURE 3.1. Projectile Inspection

SECTION IV

FREQUENCY DETERMINATION

To determine the possibility of using acoustic holography for imaging an explosive with a urethane binder, a feasibility study was conducted with the cooperation of Holosonics, Inc. [3]. The Holosonics GP-3 Imager, diagramed in FIGURE 4.1, was used. The machine is a liquid surface type imager with a frequency capability of 3, 5, 7 and 9 MHz and a maximum power output of 200 watts peak. Four types of sample materials were provided.

1. Poly B-D (urethane binder)
2. 25% Poly B-D with 75% aluminum particle inclusions
3. 25% Poly B-D with 75% glass bead inclusions
4. 25% Poly B-D with 75% halogenated wax inclusions

The materials were made up in two forms, circular wafers of two inch diameter and one-half inch thickness and 3 x 1 1/2 x 2 inch blocks encased in 1/4 inch stainless steel plates. These are shown in FIGURE 4.2. Views of each sample obtained from the GP-3 Imager are given in Appendix A.

Because of the size of the spherical glass bead inclusions, which run from 0.044 mm to 0.840 mm diameter with the major portion being approximately 0.112 mm diameter, it was determined that the lowest frequency obtainable on the GP-3 must be used. Thus, the samples were imaged at 3 MHz. This corresponds to a wavelength of 0.470 mm in fresh water, using the relation

$$\lambda = c/f \qquad (4.1)$$

where λ is the wave length, c the speed of sound in water and f the frequency. At this frequency, scattering of the ultrasound by the glass bead inclusions is significant. There are two causes for the scattering. The first is the size of the glass bead in relation to the wavelength. The bead size is approximately $\lambda/4$ at 3 MHz. This, coupled with the fact that glass has a density roughly four times that of the urethane binder, giving the glass-urethane interface a high impedence mismatch according to the relation

$$z = \rho c \qquad (4.2)$$

where z is the acoustic impedence and ρ the density of the glass, yields a transmitted beam with an extremely reduced amplitude. The acoustic impedence of the urethane is approximately that of water, so that $A_w = 1.54 \times 10^6$ kg/m^2.sec, and $Z_g = 12.9 \times 10^6$ kg/m^2. sec. Since the transmitted acoustic power is

$$a_t = \frac{4 Z_w Z_g}{(Z_w + Z_g)^2}$$

for ultrasound at right angles to the medium, only 38.3% or 76 watts is transmitted. This figure does not include losses due to Rayleigh scattering, proportion to $1/\lambda^4$, which are significant for particles less than a wave length in size. It also does not include the fact that the beam received at the liquid surface has been scattered by the glass beads and is no longer well focused.

In order to properly image the glass bead simulant, the frequency must be lower than 3 MHz. Sound is attenuated in solids according to the relation

$$A \exp(-2\pi a f x) \qquad (4.3)$$

where a is the attenuation and includes scattering effects, f is the frequency and x is the distance traveled in the medium. Attenuation measurements, data for which are given in Appendix B, show that attenuation of the ultrasound is up by a factor of 72 at 2.25 MHz in the glass bead simulant as compared to a solid, Poly B-D reference sample. Ultrasound at 3 MHz will penetrate a 1/8 inch thick glass bead sample. Measurements made at 2.25 MHz using 1/2 inch thick samples determined the attenuation ratio of 1:72 for the glass beads. Comparing the exponents of (4.3),

$$\frac{\alpha f_1 x_1}{\alpha f_1 x_1} = \frac{\alpha f_2 x_2}{\alpha f_3 x_3} \qquad (4.4)$$

f_1 = 2.25 MHz, x_1 = 1.27 cm, f_2 = 3 MHz, x_2 = 0.325 cm and x_3 = 5.00 cm. With α_p and α_g the attenuation factors for Poly B-D and the glass simulants, f_3 is determined to be approximately 0.2 MHz. Holographic images have been recorded at this frequency, showing that it will be possible to image the glass bead simulant.

Although glass beads in urethane have been used to simulate the density and weight of the explosive and are quite adequate, acoustically, they are a poor simulant for PBXW-106. The RDX inclusions in the Poly B-D have nearly the same acoustic properties as the urethane. The acoustic velocity change is small and thus interface problems are greatly reduced. The RDX inclusion size is roughly the same as the glass bead size so that the diameter to wavelength relation is not changed. Because the interface problem is reduced in the explosive, it was determined that the pure Poly B-D samples were the best acoustic simulants available.

The GP-3 Imager, operating at 3 MHz and 200 watts peak power, with a 60 cps pulse rate and 30 μs pulse width was used to image both the 1/2 x 2 inch diameter wafers with programed flaws and the 3 x 1 1/2 x 2 inch block in and out of the stainless steel case. These samples are shown in FIGURE 4.3. In the block only, through the 2 inch width, holes of diameter 0.050 inch were invisible. After glueing the block to the stainless steel with epoxy, the holes were still visible as were unbonds between the stainless and the block. This image is shown in FIGURE 4.4. Using this data with relation (4.3) determines that at 1 MHz the liquid surface imager is capable of penetrating 6 inches of the Poly B-D.

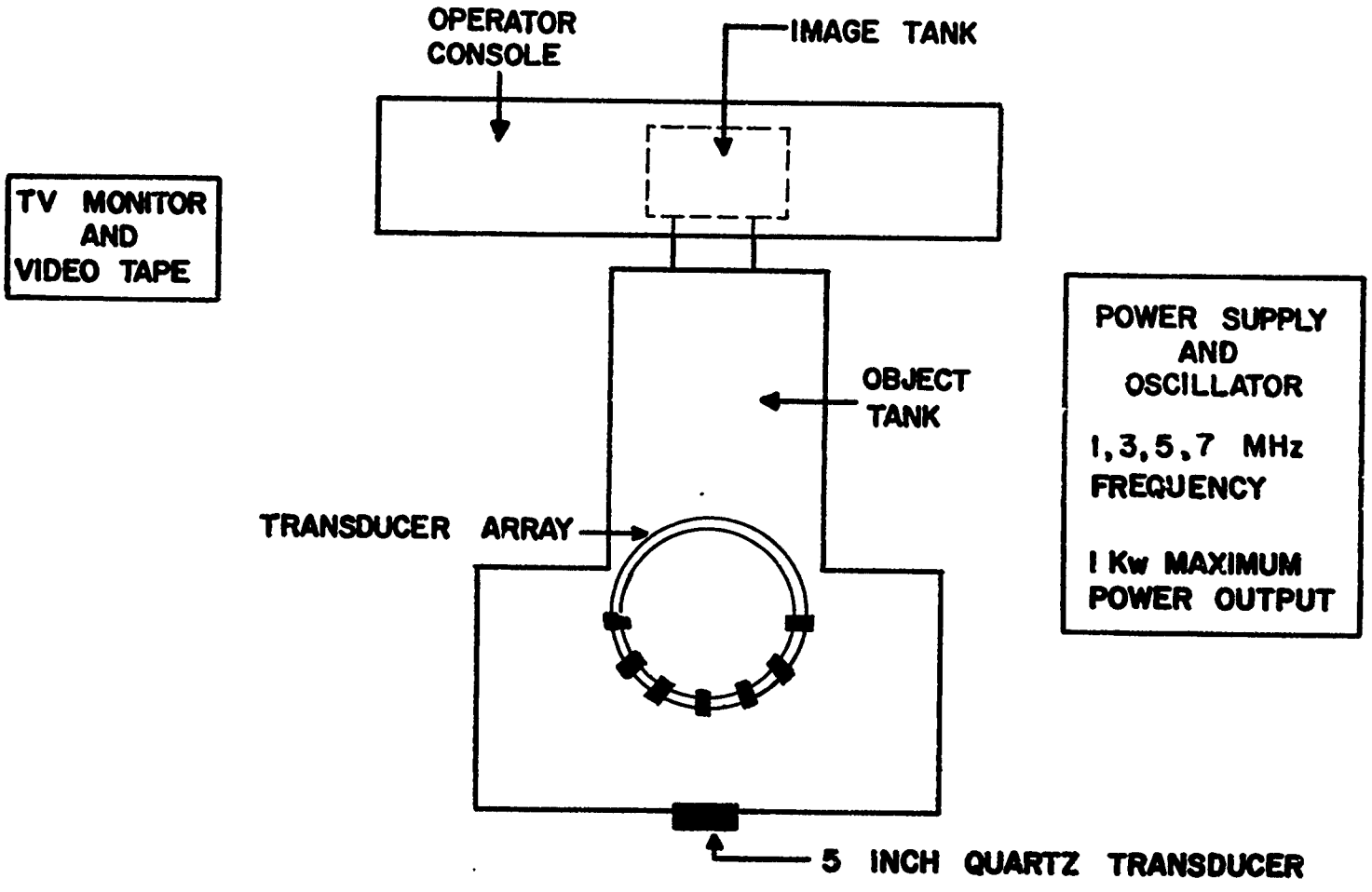

FIGURE 4.1. Acoustic Imaging System

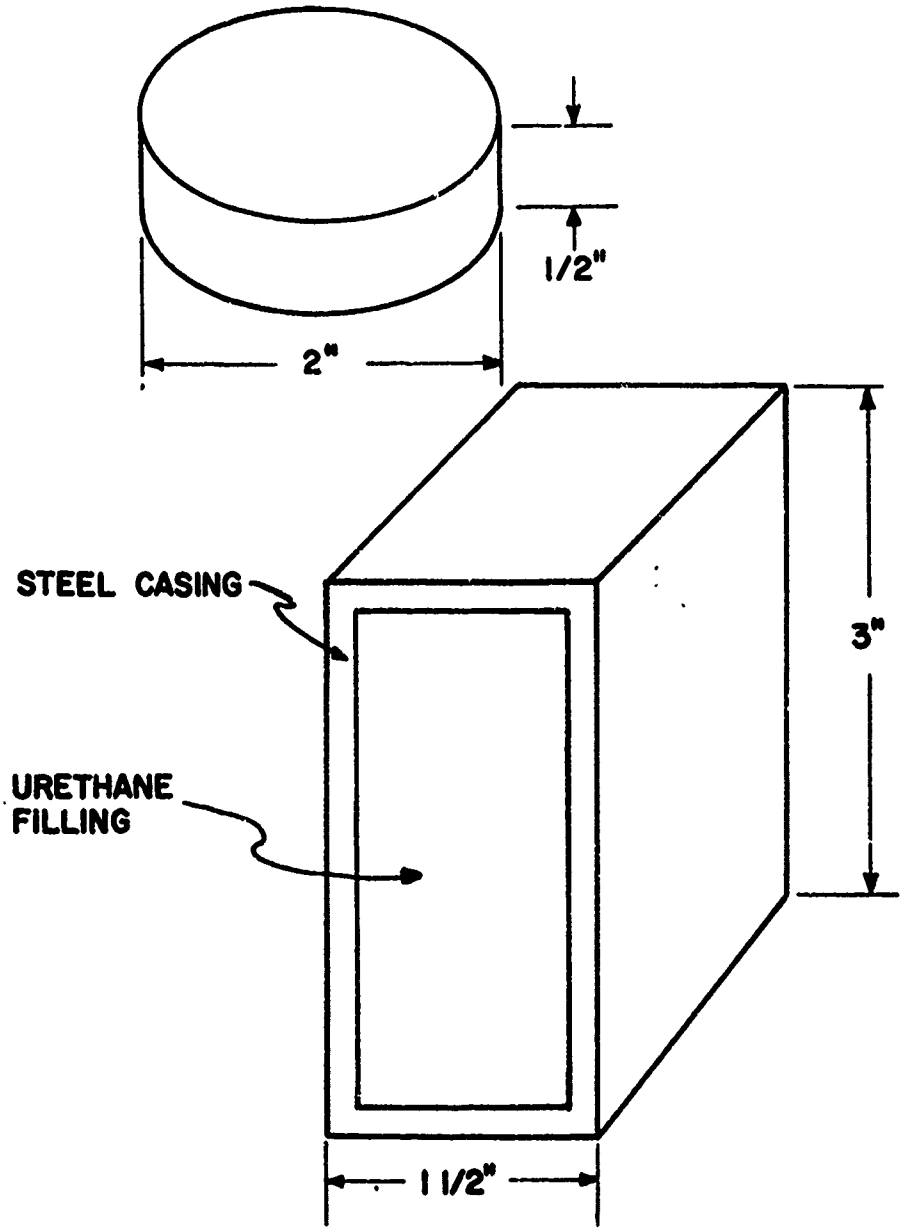

FIGURE 4.2. Circular disk and square block sample.

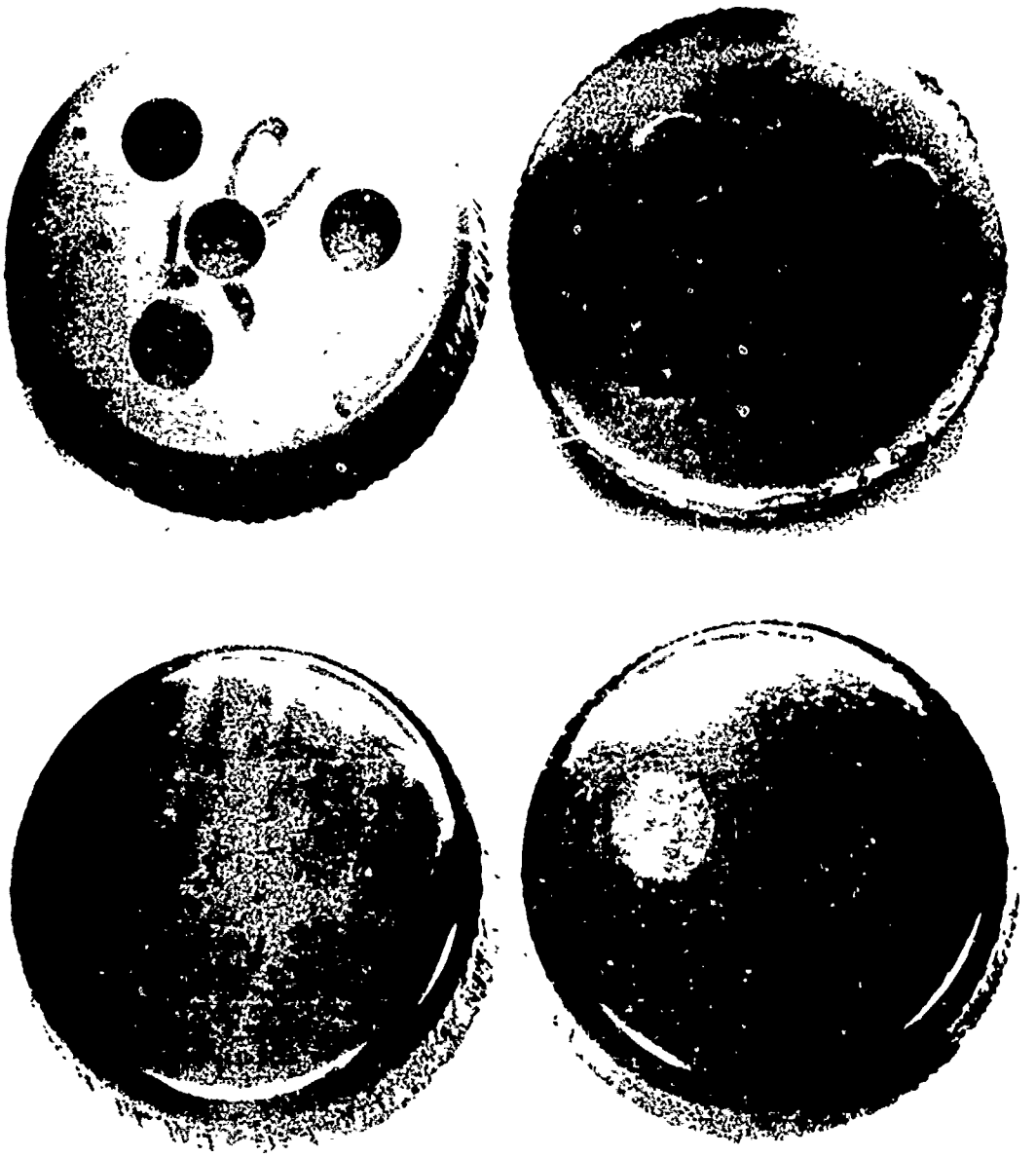

FIGURE 4.3 [illegible], alumina dart [illegible] in urethane binder with [illegible] holes; upper right, [illegible] in urethane binder with [illegible]; lower left, urethane with graduated holes, 1/16 [illegible] inch; lower right, urethane with air bubbles, 3/16 [illegible] 1/8 inch holes.

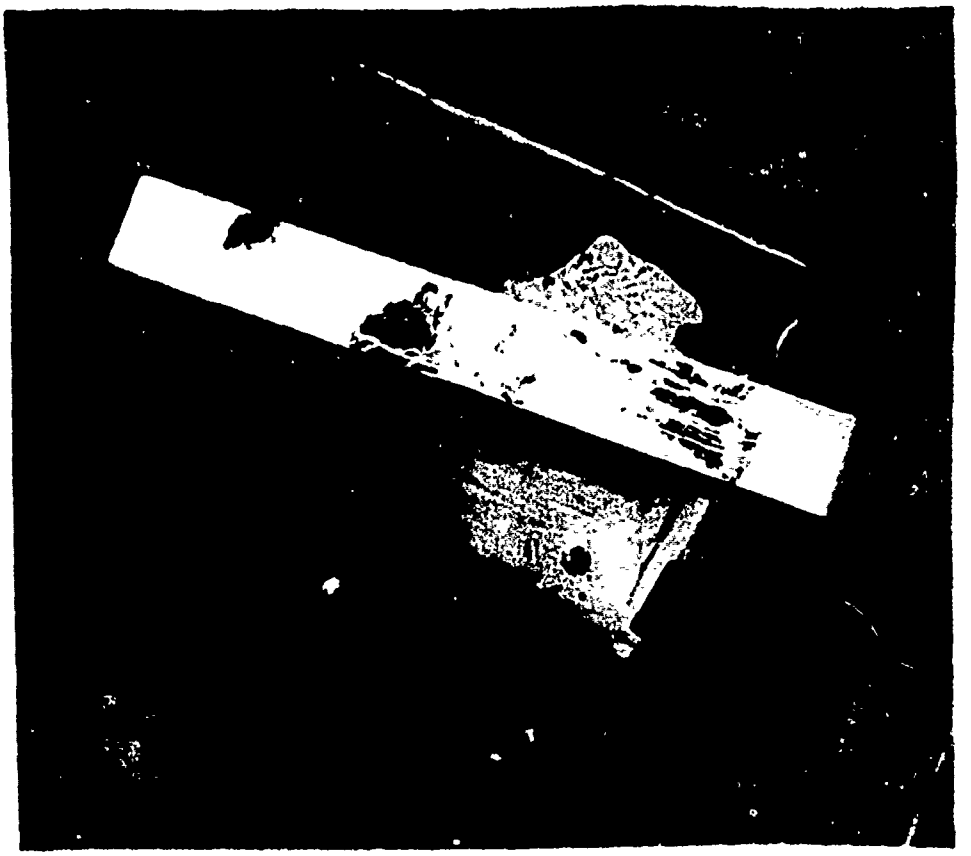

FIGURE 4.3 (b): Urethane block at back and front and programmed flaws graduating from 1/16 inch to 1/64 inch.

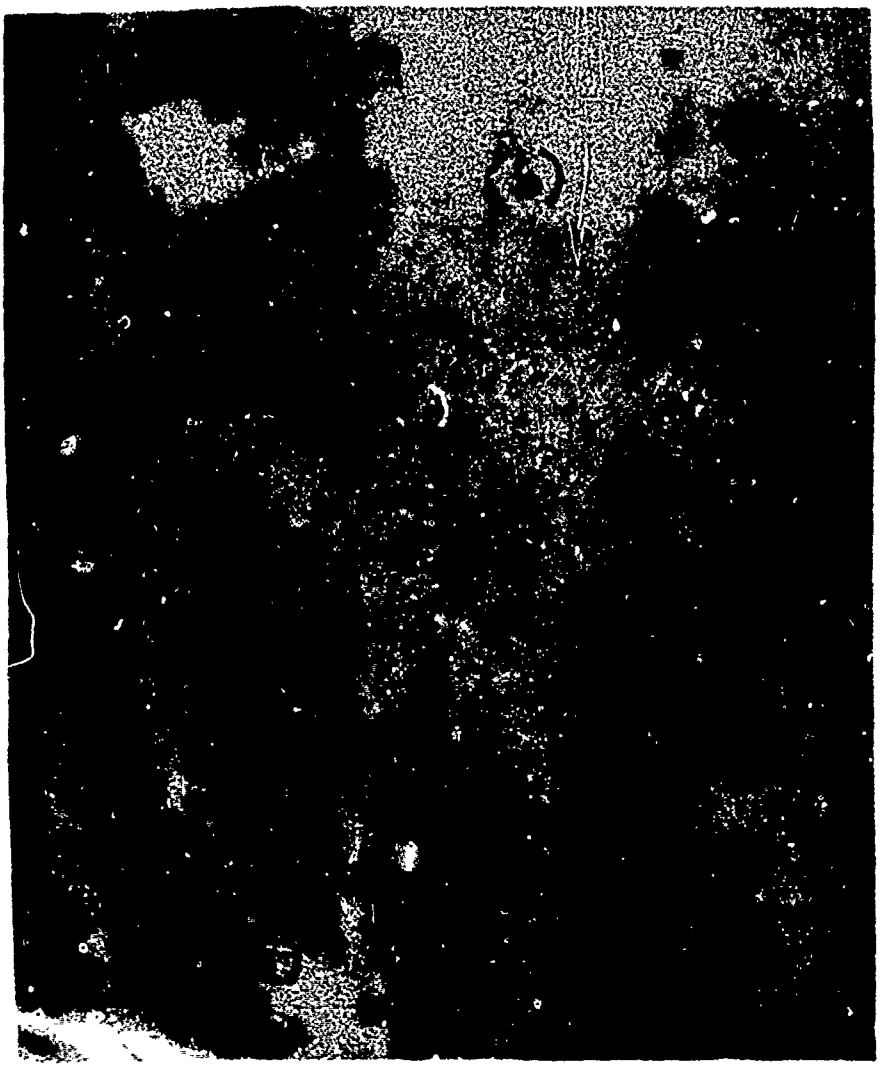

FIGURE 4.4: Ultrasonic image of block shown in Figure 4.3 (b). The dark areas designate penetration of the ultrasound, the light areas show blockage of the sound. (a) designates a hole and (b) an unbonded area. The central area of the figure shows the vertical aluminum strip.

SECTION V

TOTAL INSPECTION

The images produced of the Poly B-D block show that it is possible to detect unbonds between a metal and urethane material. The area of the unbond is no more than an air gap between the two materials and serves as an absorber of the ultrasound. This would seem to imply that if there is an air gap between the explosive billet and the metal enclosure, holographic imaging of flaws in the total projectile would be questionable. No data were obtained to determine how large an air gap the system will tolerate. This will be investigated in future work.

The determination of structural faults within a metal and unbonds at interfaces using acoustical holography has been extensively studied [1,2,4]. The GP-3 Imager at 3 MHz and 200 watts peak power in pulsed mode can determine structure faults in 18 inch thick steel plates [4] again with resolution dependent only on frequency and sound velocity in water. Table I gives frequency and wavelength relations.

Fresh water (20° C)
$\rho = 998$ kg/m^3
$c = 1481$ m/sec

f (MHz)	λ (mm)
0.25	5.924
0.50	2.962
1.00	1.480
3.00	0.470
5.00	0.296
7.00	0.211
9.00	0.165

TABLE I

Table I also shows that a frequency of 0.25 MHz will image flaws as small as .020 inch, well within the 0.125 inch tolerance necessary for the explosive billets.

SECTION VI

ELECTRONIC IMAGING SYSTEM

The liquid surface - laser imaging technique used to obtain the explosive simulant images gives excellent resolution and sensitivity, but is not practical for use in a production line device, nor in systems where high acoustic powers are necessary. Two basic electronic imaging systems are presently being considered. The first is a vidicon scan unit [5,6] and the second a hydroacoustic image transducer [7]. With either of these units it will be possible to eliminate the need for an operator of an inspection unit and total storage of all data is possible.

The vidicon scan is based on a system developed by Sokolov, using a vacuum tube with a quartz transducer face plate which is scanned by an electron beam. A total system has been developed by Bendix Research Laboratories [9] and is termed the Ultrasonic Camera. It is illustrated in FIGURE 6.1. To make this system applicable to the 5 inch projectile, the two ultrasonic transducers used for insonification are replaced by the transducer array illustrated in FIGURE 6.2. The transducers are arranged on the holder for optimum insonification of cylindrical objects. The insonifying beam will be at an angle as near 90^{o} to the object as possible. This is accomplished by a series of mirrors arranged to reflect the ultrasound towards the object or by a varying voltage input to each of the transducers in the array. The transducers on the array are in phase and are air backed. The beam, after transmission through the object, is focused on the face of the vidicon tube by a variable focus lense which is described by Knollman, Bellin and Weaver [10].

If the vidicon tube system is used, the quartz face plate will be replaced by a face plate incorporating a ceramic mosaic. The ceramic plate is silvered on the inner surface where it is scanned by the electron beam. The cuts for the mosaic are made on the outer surface of the ceramic and are filled with an insulating potting compound. The potting serves as a reinforcement so that the face plate can withstand the outer water pressure against the evacuated interior. The size of the mosaic elements is determined by the wavelength of the ultrasound used for insonification. For a frequency of 1 MHz, a typical element size

is 1.5 mm^2. The width and depth of the cuts are determined by the type of ceramic used. Typically, the cut depth is approximately one half the thickness of the ceramic. The ceramic plate, before the mosaic is cut, is 1 MHz in thickness. A change in the frequency of the ceramic is expected after the cuts are made. This can be compensated by using a variable focal length lense.

The vidicon system described must be stationary, thus to image an entire projectile, the projectile would be moved through the ultrasound beam. Using the ceramic mosaic face plate is advantageous over the quartz plate described by Fritzler et. al. At 1 MHz, the thickness of the quartz is not sufficient to allow use of a large aperture face plate without some form of bracing. This bracing is visible in the reconstructed image. The ceramic mosaic requires only the potting in the cuts for bracing and, because of the size of the cut in reference to the wavelength, this is not visible in the image. The disadvantage of using the ceramic mosaic is economic. A 150 mm plate would contain 10,000 elements. Machining costs would be prohibitive.

A non-vacuum system, such as the hydroacoustic system developed by Knollman et. al. [9] has several advantages over the vidicon device. It is more easily maintained and there is no problem encountered in mounting the ceramic mosaic to withstand pressure differences. In fact, rather than a square mosaic, a linear mosaic is used. A diagram of such a mosaic is given in FIGURE 6.3. One method of fabricating a mosaic of this type is given by Knollman and Brown. The size of the cuts and the elements again governs the resolution. The mosaic fabricated by Knollman, et. al. [8], corresponds to an f/2 lense in water at 2.5 MHz. The cuts are 0.38 mm in width and 0.25 mm in depth. Each element is 1.65 mm^2. The linear mosaic is coupled with a mechanical mirror scan to allow a view of an area as large as the acoustic lens system. The lens size is not restricted. Its focal length is determined by the frequency of the linear mosaic. The usable beam width of the insonifying array is made comparable to the size of the lens. The scan speed of the system is limited by the mechanical scan.

For the purpose of production line testing, investigations made of both the vidicon and linear mosaic indicate that the latter is more suitable. Both are limited in speed by a mechanical movement of either the projectile or the sound beam. However, movement of the sound beam can be done electronically and will thus speed up the scan rate. The lesser cost of the linear

mosaic production also makes it more attractive. An additional advantage of the linear mosaic is that it can be incorporated with the acoustic lense to form a portable imaging system making it ideal for underwater detection work.

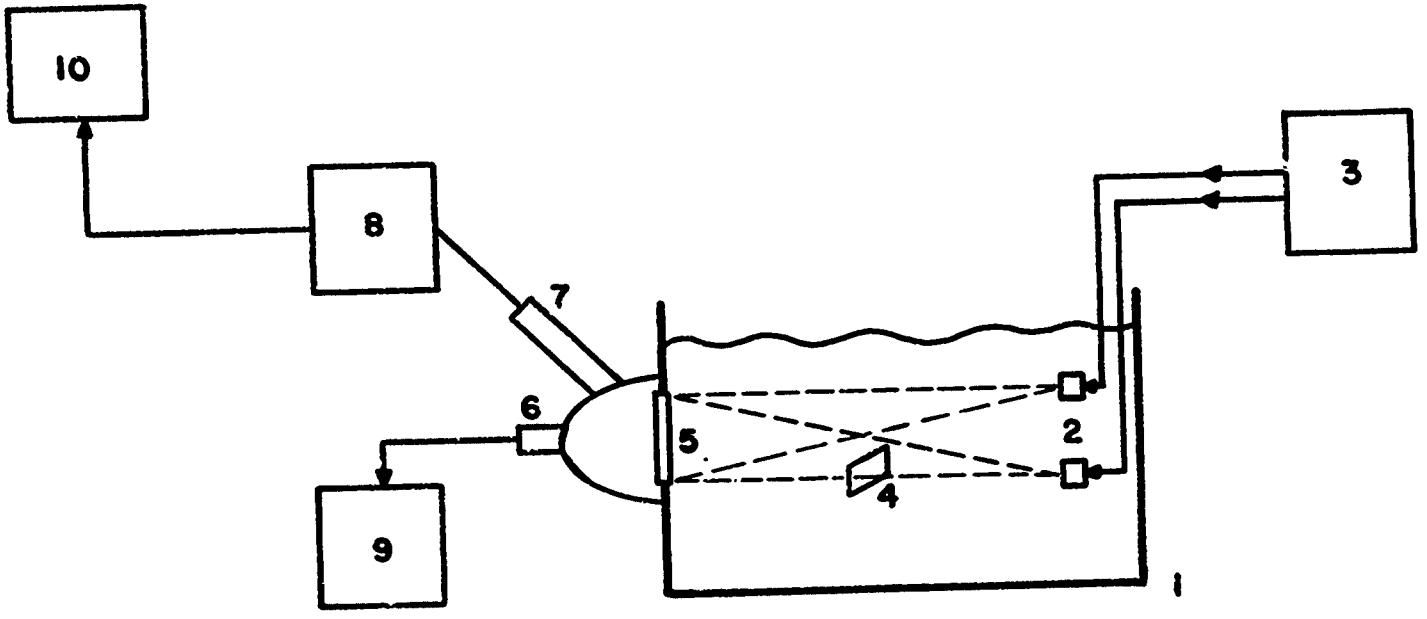

FIGURE 6.1. Immersed in the water tank (1) are two ultrasonic transducers (2) fed by generator (3). The beams are impinging upon quartz target (5) after one of the beams was scattered by target (4). The electron beam in cathode ray tube (6) induces secondary emission multiplied by electron multiplier (7) and carrier amplifier (8) and finally displayed on TV monitor (10). Box (9) includes the electronic circuits for beam generation and deflection.

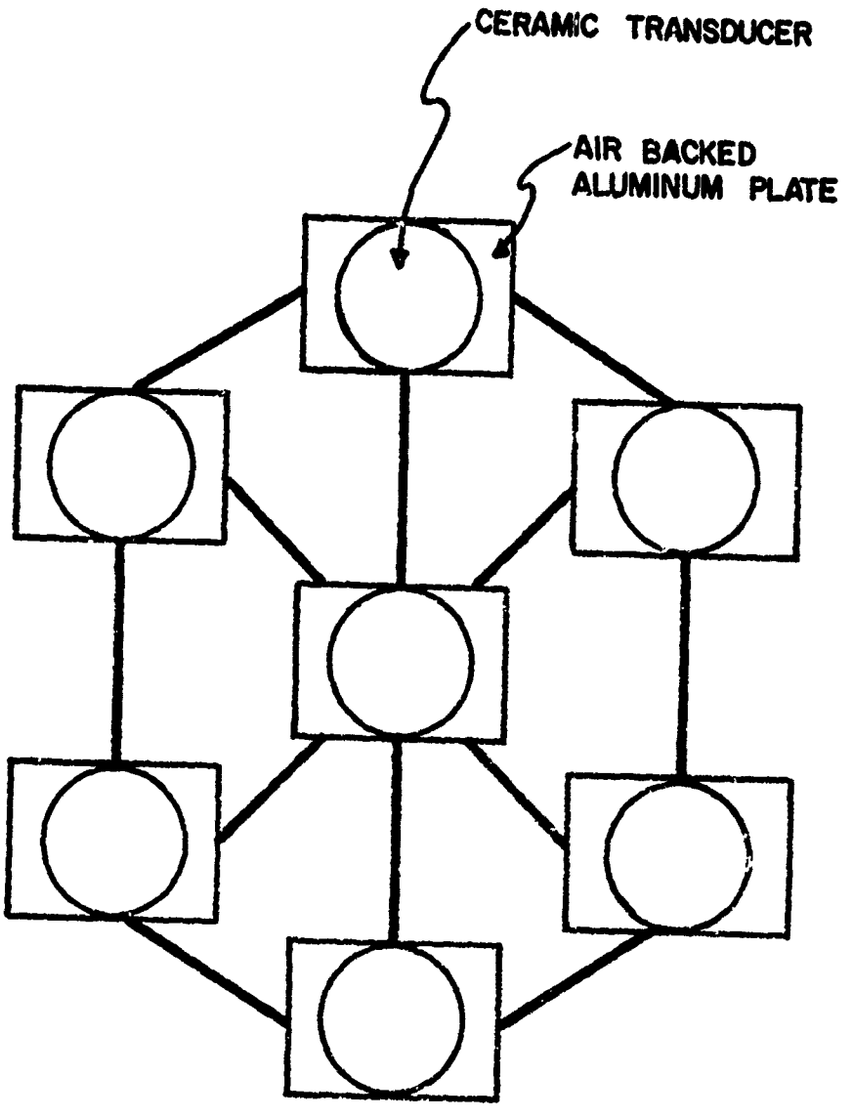

FIGURE 6.2. Sonifying array. The elements have round ceramic transducers mounted air-backed.

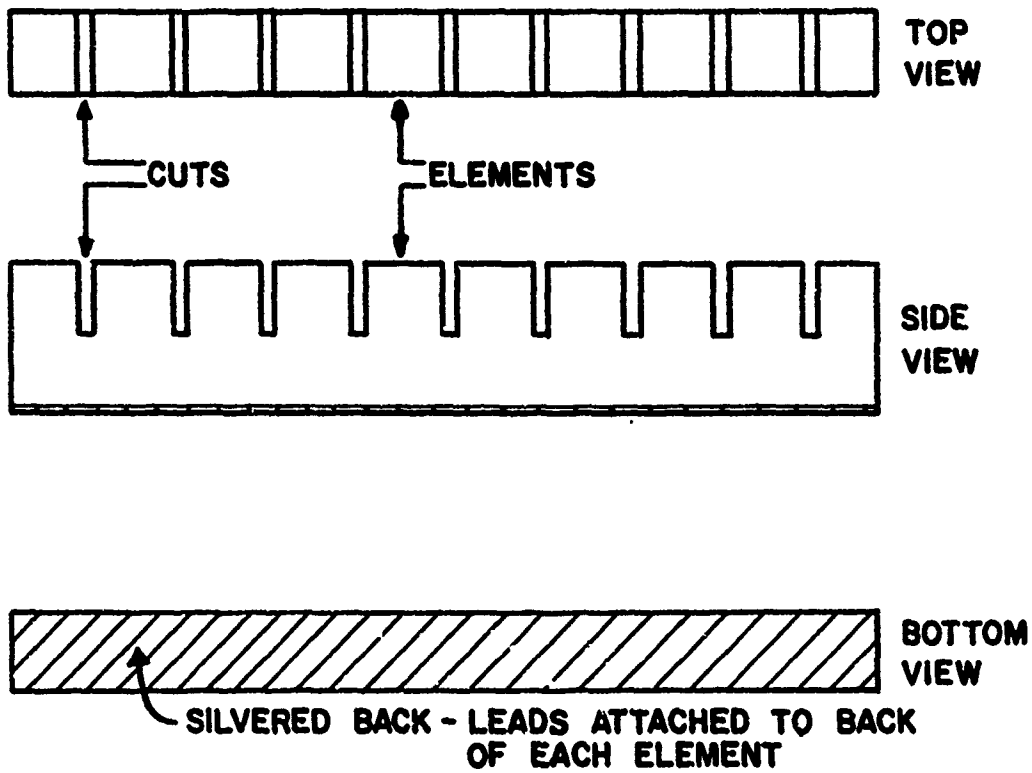

FIGURE 6.3. Linear mosaic. Elements are cut to the 1 MHz frequency.

SECTION VII

USES OF ACOUSTIC IMAGING SYSTEMS

Acoustic imaging can be divided into two areas of application; low frequency (1-30 MHz), high penetration of the test medium with low resolution, and high frequency (30-100 MHz) low penetration of the test medium with high resolution. The applications in both areas are numerous. Below are listed several of the most obvious. These by no means exhaust the list.

Low Frequency (resolution up to .009 inch)

1. Detection of flaws and density differences in explosives and solid rocket propellants.
2. Weld inspection where tolerances are large.
3. Detection of cracks in metal, fiberglass or plastic pipe with portable units.
4. Mineral detection by change in strata or heat content.
5. Medical applications where large areas of high density material are involved, including internal bone studies.
6. Underwater detection of buried objects.
7. Inspection of damaged electronic components.

High Frequency (resolution up to 20μ)

1. Metallic structures and internal cracking.
2. Phase changes.
3. Biological samples.

Most applications of the work listed above are in development stages and very little production equipment is available. At the Naval Weapons Laboratory, work is being pursued in the field of solid rocket propellants and large bone area inspection. This work is being done at power levels of over 400 watts peak and at frequencies ranging between 1 and 3 MHz. A liquid surface unit is being used at present but major application of imaging techniques will be done with an electronic sensor. Several successful attempts have been made to image soft tissue in the hand and forearm. Tendons and muscle structure are clearly visible. An example of the images obtained is given in FIGURE 7.1. The liquid surface unit operating at 3 MHz has proved quite acceptable for this work, although improvements must be made.

The prototype unit to be used for inspection of the cylindrical explosive loads will be equally applicable to metal, plastic, or fiberglass pipe inspection because of its high power capability. The linear mosaic heads in the receiver and the elements used in the sonifying array are removable so that frequency changes can be easily made. In addition, investigation is being made into a tunable transmitter and receiver in the 1 to 5 MHz range. This would enable a rough inspection for gross flaws and, where necessary, a rapid conversion to a high frequency for better resolution. A method has also been devised whereby this unit can be made portable. Underwater detection of buried objects is made possible by an underwater camera now in use by the Navy and developed by Lockheed Research and Development Center. More development work is also necessary here for higher resolution and greater penetration of bottom ooze.

In the high frequency range, Zenith has developed a 100 MHz unit which has been used for inspection of thin, biological samples. The unit has been used to check samples of iron and mishmetal from the Naval Weapons Laboratory. Now controlled experiments are necessary to determine full capability of the unit, but grain structure in the 10 mil thickness samples appeared to be visible. No unit of this type is available in-house, but further development at Naval Weapons Laboratory in the high resolution area would be advantageous.

By the above discussions it is evident that further effort in the area of acoustic imaging by Naval personnel would be quite advantageous in many fields. Hopefully, work can continue at the Naval Weapons Laboratory to explore fully the possibilities in all fields and perfect the state-of-the-art techniques now available. This will greatly assist the transition from the laboratory to the production plant.

FIGURE 7.1(a): The top view is an ultrasonic image (negative) of a normal hand showing the tendon structure between the thumb and forefinger. The image was obtained using 3 MHz sound at 300 watts peak power. The lower image is the same view of a hand (positive) with silastic sheaths on the tendons.

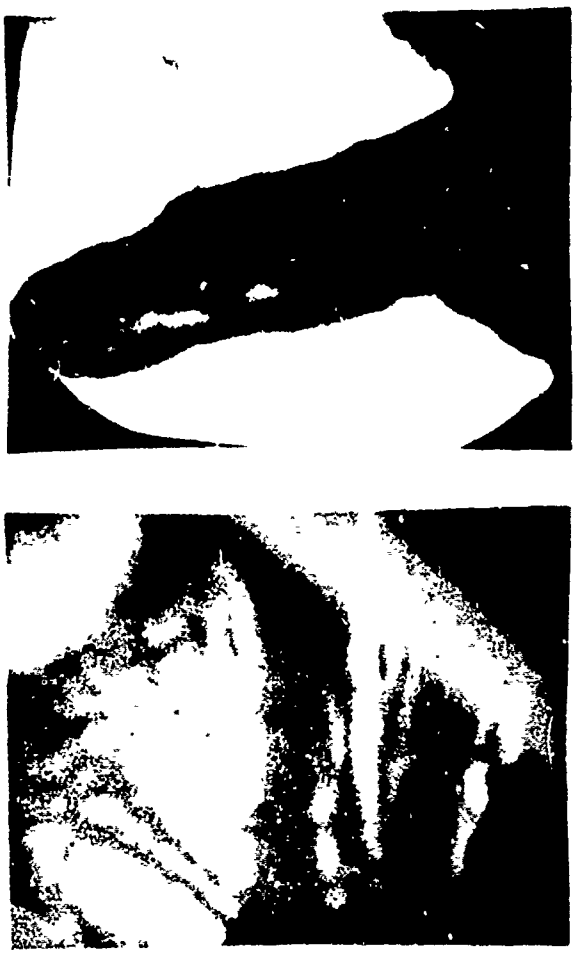

FIGURE 7.1(b): The upper view is an ultrasonic image of the forefinger showing the silastic tendon sheath in the lower part of the finger. The lower view shows the entire tendon structure in the thumb and forefinger area.

SECTION VIII

BIBLIOGRAPHY

1. "Preliminary Report of Application of Ultrasonic Imager to the Petroleum Industry Test Samples", submitted by Standard Oil Company of California, Richmond, California, March 10, 1971.

2. "New Techniques for Real-Time Acoustic Holographic Images", proposal brief, Lockheed Research Laboratory, Palo Alto, California, November 19, 1971.

3. V. Neely and B. Brendon, private communication, September, 1971.

4. J. L. Kreutzer and P. E. Vogel, "Acoustic Holographic Techniques for Nondestructive Testing", in Acoustic Holography, Vol. I, (ed., A. F. Metherell, H. M. A. El-Sum, L. Larmore), Plenum Press, New York, (1969) 73.

5. J. L. DuBois, IEEE Trans. on Sonics and Ultrasonics, Vol. SU-16, 3, (1969) 94.

6. S. Sokolov, "Means for Indicating Flaws in Materials", U. S. Patent 2,164,125.

7. P. S. Green, J. L. S. Bellin and G. C. Knollman, J. of Ac. Soc. of Am., 44, (1968) 1719.

8. D. Fritzer, E. Marom, and R. K. Mueller, "Ultrasonic Holography via the Ultrasonic Camera", Acoustic Holography, Vol.I, 249.

9. G. C. Knollman, J. L. S. Bellin, and J. L. Weaver, J. of Ac. Soc, of Am., 49, (1971) 253.

10. G. C. Knollman and A. E. Brown, Rev. of Sci. Inst., 42, (1971) 1202.

APPENDIX A

VIEWS OF SAMPLES OBTAINED FROM THE GP-3 IMAGER

The views shown are ultrasonic images of the samples discussed in the text. The images in the lower portion of FIGURE A.1 were obtained from Holosonic's GP-3 Imager operating at 3 MHz and 200 watts peak power. The images in the upper portion of the figure were obtained on the ultrasonic imager at the Naval Weapons Laboratory operating at 3 MHz and 400 watts peak power. The additional power was necessary to penetrate the alumina and glass bead samples.

FIGURE A.1: Ultrasonic images of the samples shown in Figure 4.3 (a). Position of the samples corresponds to that in Figure 4.3 (a). The dark areas show the voids in the samples.

FIGURE A.2: Mishmetal cylindrical liners. The left hand image used a cylindrical transducer; the right hand, a flat transducer. Cracking is shown. The cylindrical transducer yields a more well defined image.

APPENDIX B

ATTENUATION MEASUREMENTS AT 2.25 MHz AND 1 MHz

Shown are pulse-echo measurements in FIGURES B.1 to B.4, and through-transmission measurements in FIGURES B.5 to B.8. The samples used were those shown in FIGURE 4.3(a). Pulse-echo data was taken at 2.25 MHz. Through-transmission data was taken using a continuous wave at 1 MHz.

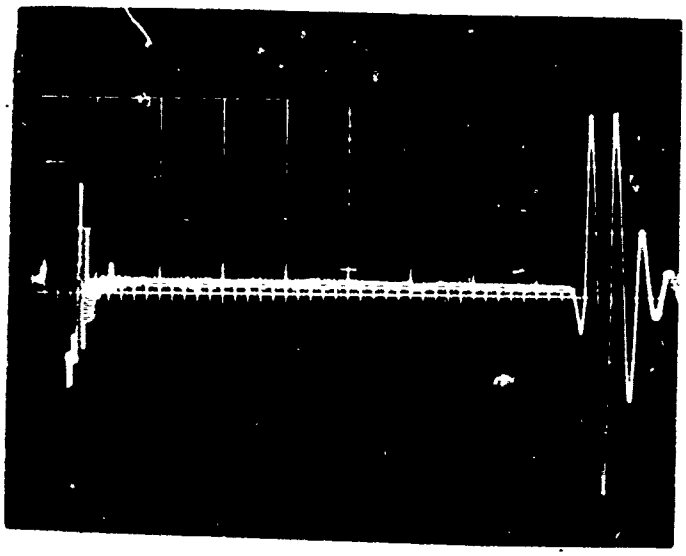

FIGURE B.1: Sample: Pure urethane longitudinal phase velocity 1538 m/sec. Time base: 1 μs/cm. Amplitude of received pulse: 5.8 cm. Receiver gain = 1. Frequency: 2.25 MHz.

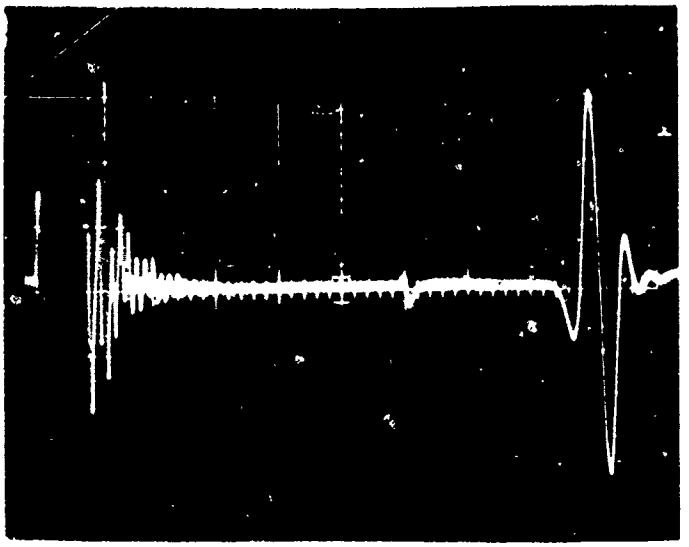

FIGURE B.2: Sample: Aluminum Powder Urethane. Phase Velocity 1540 m/sec. Time base: 1 μs/cm. Amplitude of the received sound pulse = 6 cm. Receiver gain = 10. Attenuation @ 2.25 MHz with respect to the urethane: 1/10

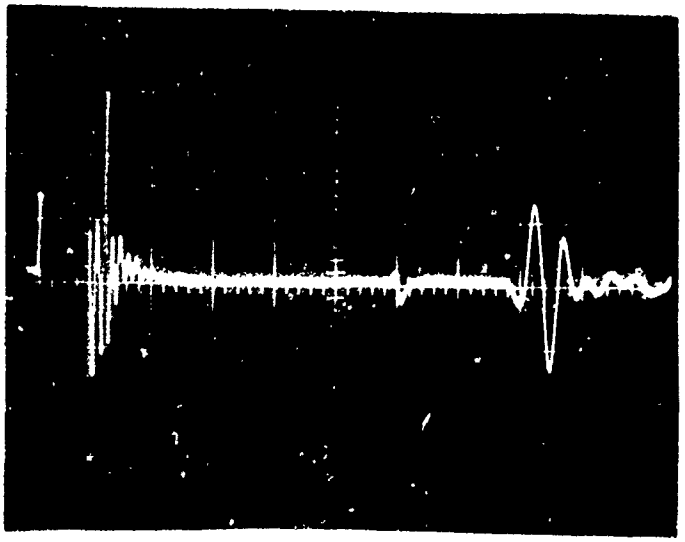

FIGURE B.3: Sample: Halogenated Wax in urethane. Phase Velocity = 1630 m/sec. Time Base 1μs/cm. Amplitude of the received sound pulse = 2.6 cm. Receiver Gain = 10. Attenuation at 2.25 MHz with respect to the urethane = 1/22.

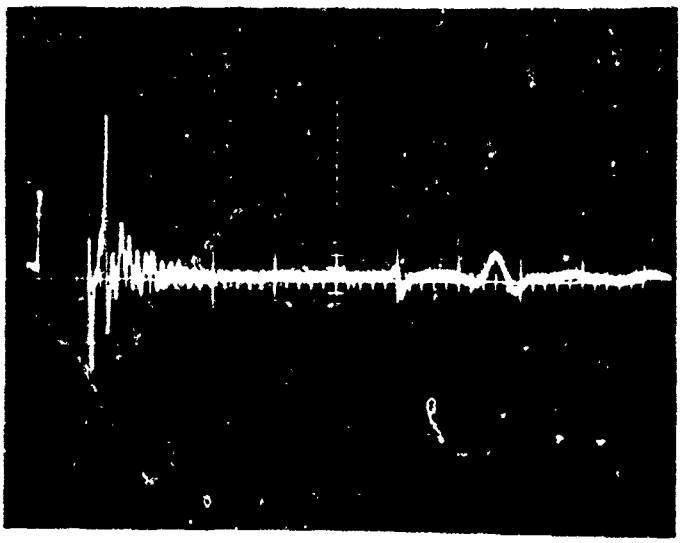

FIGURE B.4: Sample: Glass Beads in Urethane. Phase Velocity 1820 m/sec. Time Base 1 μs/cm. Amplitude of the received sound pulse = 0.6 cm. Receiver 6 cm = 10. Attenuation @ 2.25 MHz with respect to the urethane = 1/72.

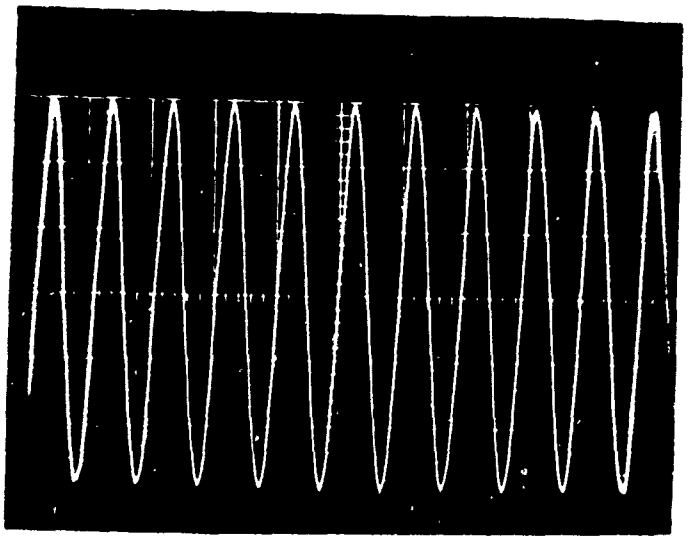

FIGURE B.5: Sample: Pure Urethane. Frequency 1 MHz. Receiver Gain = 1.

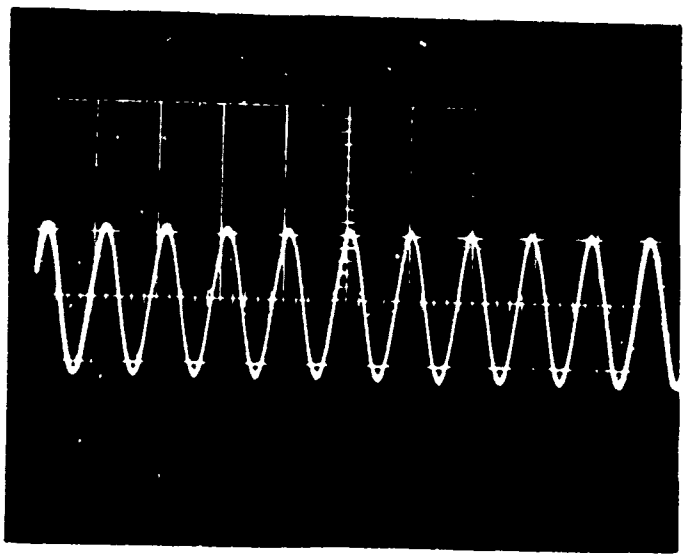

FIGURE B.6: Sample: Aluminum Powder/Urethane. Frequency 1 MHz. Receiver Gain = 1. Attenuation amplitude with respect to the urethane = 1/2.72.

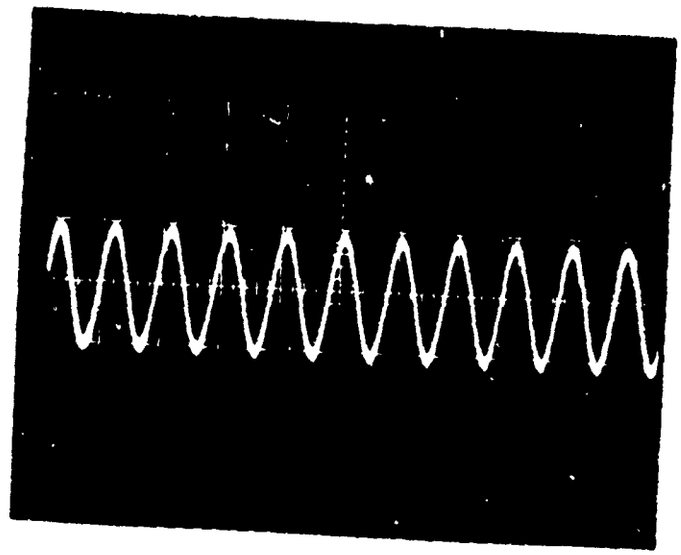

FIGURE B.7: Halogenated wax in urethane. Frequency 1 MHz. Receiver Gain = 1. Attenuation amplitude with respect to the urethane = 1/7.1

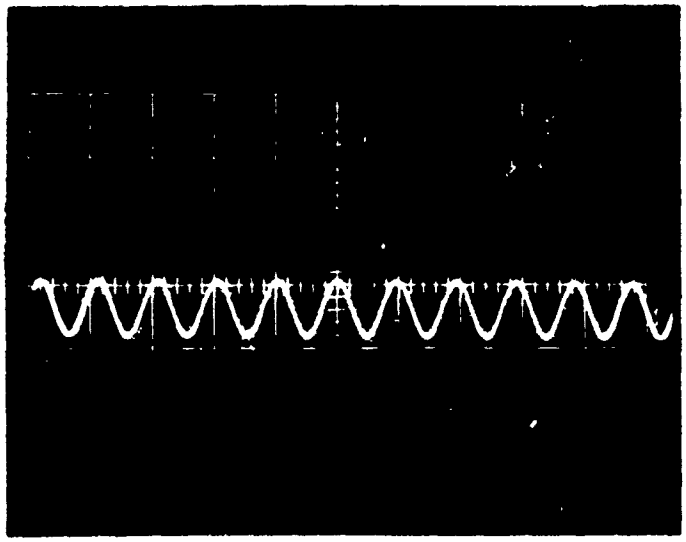

FIGURE B.8: Sample: Impregnated glass beads. Frequency 1 MHz. Receiver Gain = 10. Attenuation with respect to the clear red sample = 1/27.3.